Materials Advances

ROYAL SOCIETY OF CHEMISTRY

COMMUNICATION

View Article Online
View Journal | View Issue

Cite this: *Mater. Adv.*, 2021, 2, 4240

Received 9th February 2021,
Accepted 9th May 2021

DOI: 10.1039/d1ma00121c

rsc.li/materials-advances

A binary PMMA/PVDF blend film modified substrate enables a superior lithium metal anode for lithium batteries†

Xiaosong Xiong, Ruoyu Zhi, Qi Zhou, Wenqi Yan, Yusong Zhu,* Yuhui Chen, Lijun Fu, Nengfei Yu* and Yuping Wu*

Metallic lithium is a promising next generation electrode material due to its ultrahigh specific capacity and lowest redox potential. However, its short cycling lifespan and safety hazards have hindered its practical application. To improve the cycling performance of lithium metal anodes, dendrite-free lithium deposition and a stable electrode–electrolyte interface are of vital importance. Here, we prepared a thin PMMA/PVDF gel coating using an electrospinning technique on a Cu substrate as the anode directly, which can not only homogenize lithium ion flux, promoting uniform lithium deposition, but can also alleviate the dramatic volume change in the lithium anode, improving the stability of the electrode interface. Owing to the excellent lithiophilic properties and high mechanical flexibility of the binary blend polymer coating, stable cycling for over 1400 h is achieved in a Li/Li symmetric cell using modified coating at 1 mA cm^{-2} with a cycling capacity of 1 mA h cm^{-2}. The binary blend polymer coating with complementary properties prepared by this facile method provides a new insight for the lithium metal anode improvement.

1. Introduction

Recent developments in consumer electronics and electric vehicles have intensified the need for rechargeable batteries with high energy density and long cycling life.[1,2] Compared with the graphite anode of commercial lithium ion batteries, lithium metal anode has been attracting considerable interest due to its high theoretical specific capacity (3860 mA h g^{-1}) and lowest redox potential (−3.04 V *vs.* SHE).[3] However, the problem is that the low coulombic efficiency and poor cycle life originating from uneven lithium deposition during cycling hinder the practical performance of lithium metal anodes.[4] To be specific, owing to the high reactivity of lithium metal, a solid electrolyte interface (SEI) is formed on the anode surface spontaneously upon contact with the electrolyte. However, the fragile SEI can hardly withstand the dramatic volumetric change of the lithium metal anode during the charge/discharge process, and thus cracks form on the SEI. As a result, the exposed fresh lithium comes in contact with the electrolyte to repair the SEI by side reactions; this repeated process will cause a great loss in active lithium and electrolyte subsequently, and lead to inhomogeneity in SEI composition. Furthermore, the local inhomogeneity in the composition and structure of SEI would give rise to an uneven and loose lithium deposition layer due to the nonuniformity of lithium ion flux on the SEI surface, which is favorable for the evolution of lithium dendrites. On one hand, the electrical contact between lithium dendrites and substrate could be broken to form ''dead lithium'' gradually, increasing the interface resistance and shortening the cycle life significantly. On the other hand, there is every probability that dendrites will pierce through the separator and cause an internal short-circuit, posing safety hazards.[5,6] Therefore, a stable electrode/electrolyte interface and dendrite-free lithium deposition morphology are critically important for high efficiency lithium metal anode with a long life-span.

To date, a variety of methods have been developed to improve lithium metal batteries, which mainly include modifying electrolytes such as adding additives,[7] using solid electrolytes,[8] applying a protective coating on the separators[9] or the surface of anode directly,[10] and providing host materials.[11] Generally, the enhanced SEI formed *in situ* by electrolyte modification cannot achieve ideal mechanical robustness to endure the dramatic volumetric change of lithium anode, while mechanically suppressing the dendrites by solid electrolyte also results in poor interface contact. As a result, more recent attentions have been focused on the electrode surface modification, and coating layers with great flexibility and mechanical strength exhibit the ability to stabilize the electrode interface.[12,13] Generally, high ionic conductivity and sufficient

State Key Laboratory of Materials-oriented Chemical Engineering & School of Energy Science and Engineering, Nanjing Tech University, Nanjing 211816, China. E-mail: zhuys@njtech.edu.cn, yunf@njtech.edu.cn, wuyp@fudan.edu.cn

† Electronic supplementary information (ESI) available. See DOI: 10.1039/d1ma00121c

mechanical robustness are the two essential properties for an ideal modified coating to accommodate the inhomogeneous Li^+ ion distribution near the lithium anode surface and sustain the serious electrode deformation during cycling. However, it is still a challenge to reduce the additional interface resistance and deposition barrier introduced by the modified coating, and most improvement strategies are far away from application due to high cost and complex preparation process.

In this contribution, poly(vinylidene fluoride) (PVDF) and poly(methyl methacrylate) (PMMA) are utilized to build an artificial protective coating on the Cu substrate for lithium anode *via* the electrospinning technique. The main PMMA polymer composition has the advantages of good electrochemical stability, low interfacial impedance and low cost. In addition, considering that the strong interaction between the carbonyl (-*CO*-) group in the methyl methacrylate (MMA) unit and liquid organic electrolyte, PMMA can contain a large amount of liquid electrolytes and shows superior affinity with the liquid electrolyte,[14] significantly reducing the interface resistance and lithium heterogeneous nucleation barrier, which is conducive to the uniform deposition of lithium in the following deposition process. To improve the mechanical robustness of the *ex situ* modified coating, a polyvinylidene fluoride (PVDF) matrix is added. Its characteristics of high dielectric constant (~10) and relative low surface energy (~35 mJ m^{-2}) are believed to reduce the overpotential and promote lithium to deposit compactly with a smaller area in theory.[15] Also, the –C–F– groups with strong electron-withdrawing capabilities make the matrix highly resistant to electrochemical oxidation, ensuring the superior physical and chemical stabilities of the modified coating, and maintaining the integrity of the coating. Consequently, due to the synergistic effect of the composition and structure of the modified polymer coating, Li^+ ions diffusing from the bulk electrolyte can be evenly distributed in the protective coating and get deposited on the Cu substrate compactly and uniformly. As a result, in half-cells, the PMMA/PVDF modified Cu electrodes show an enhanced coulombic efficiency of 98.3% for over 260 cycles at 1 mA cm^{-2}, and a stable cycling life-span, which is four times than that of bare Cu electrodes. In addition, low overpotential (~20 mV) is also achieved in Li/Li symmetric cells cycled at 1 mA cm^{-2} for over 1400 h when protected by the PMMA/PVDF modified coating, which is much better than that of the bare electrodes (~400 h). Furthermore, a dendrite-free lithium deposition morphology is observed on the PMMA/PVDF coating modified electrodes and thus a stable electrode/electrolyte interface is ensured.

2. Results and discussion

As shown in Fig. 1a, the PMMA/PVDF modified layer was directly deposited on the copper substrate by the electrospinning technique. Afterwards, the electrode foil was punched to obtain electrodes with a diameter of 15 mm. The thickness of the modified layer was controlled by the electrospinning time.

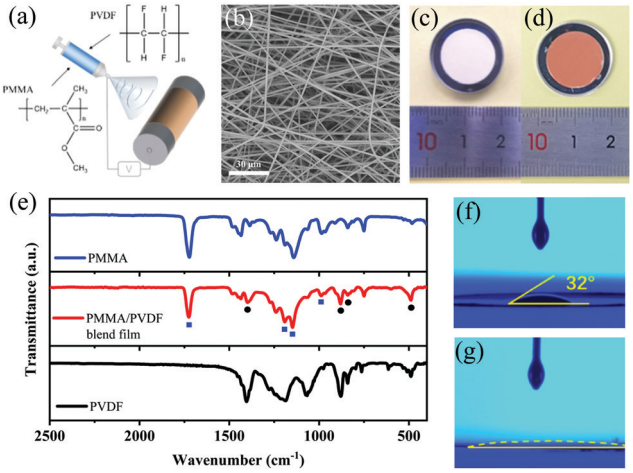

Fig. 1 Preparation and characterization of the PMMA/PVDF layer. (a) Schematic diagram of the preparation and synthesis process of the PMMA/PVDF modified coating. (b) SEM image of the modified layer. (c and d) Digital photos of the modified layer before (left) and after (right) immersion in electrolyte. (e) FTIR spectra comparison of modified coating at different states. (f and g) Contact angle images of modified and unmodified electrodes.

When measured using a digital micrometer, the optimal thickness was about 50 μm for a 5 h electrospinning. After the cell was assembled, the modified layer was compressed to 4 μm (Fig. S1a, ESI†), which ensures no additional resistance for the migration of lithium ions. Fig. 1b shows the top-view scanning electron microscope (SEM) image of the electrospun PMMA/PVDF film. A 3D interconnected network structure with a number of voids is obtained *via* the electrospinning technique, which is beneficial to store massive electrolyte, facilitates the diffusion of lithium ions and restricts lithium deposition.[16] The fibers are dispersed uniformly without beads, exhibiting an average diameter of 1.6 μm (Fig. S1b, ESI†). As is shown in the digital picture (Fig. 1c), the modified layer adhering to the Cu foil is white in colour. Subsequently, it turns into a flexible and transparent gelatinous substance as soon as it comes in contact with the electrolyte (Fig. 1d). This result can be explained by the fact that the PMMA/PVDF macromolecules swell after absorbing electrolyte.[17] Afterwards, the pristine electrospun modified coating was removed from the copper electrode for Fourier transform infrared spectra (FTIR) measurement (Fig. 1e). The characteristic peaks of PMMA and PVDF are clearly identified in the pristine PMMA/PVDF electrospun coating. The characteristic peaks of PMMA appear at 1726 cm^{-1} (C═O stretching vibration), and 988 cm^{-1} (CH_2 wagging mode). Also, the wide split bands at 1148 and 1191 cm^{-1} are from the C–O stretching vibration in PMMA. The bands at 1400 cm^{-1} (CH_2, CF_2 deformation vibration), 877 cm^{-1} (amorphous phase PVDF), 841 cm^{-1} (–CH_2 in-plane deformation vibration) and 490 cm^{-1} (wagging mode of CF_2) are from PVDF. Both compounds do not present much interaction, and thus we can determine that a uniform binary PMMA/PVDF blend coating was prepared by electrospinning successfully. The affinity of the current collector with the electrolyte was evaluated by

measuring the contact angle on the substrate (Fig. 1f and g). The contact angle of ether-based electrolyte on the Cu foil surface is about 32°. As for the modified Cu foil, the electrolyte spreads out as soon as it comes in contact with the electrode surface. This result demonstrates an improved wettability for the electrolyte on the modified anode, which is known to be able to mitigate the concentration gradient of lithium near the anode surface and decrease cell resistance.[10]

Li/Cu half cells were used to investigate the influence of PMMA/PVDF modified coating on lithium deposition/dissolution behavior. Firstly, the cyclic voltammogram (CV) of the Li/modified Cu half cell during the first three cycle range in −0.2–1.5 V is given in Fig. 2a. The reduction peak at 0.37 V in the first cycle represents the SEI formation process, and a couple of redox peaks near 0 V (*vs.* Li^+/Li) are the characteristic of the lithium deposition/dissolution process, which means that the introduction of a modified layer surely will not hinder the normal deposition and dissolution behavior of lithium. Furthermore, in the third cycle, modified Cu exhibits a higher peak height (8.99 mA) than bare Cu (4.76 mA) (Fig. S2a, ESI†); the increased peak height in the CV curves of the cell using modified electrode indicates a faster lithium diffusion behavior on the modified substrate surface,[18] confirming that a good SEI was achieved. In order to demonstrate the positive regulation of the modified coating on lithium deposition behavior, the overpotential of Li deposition in the first cycle was investigated, which is defined as the difference between tip voltage (lithium nucleation overpotential) and the later stable plateau voltage (mass transfer overpotential) in the voltage curve during the discharge process. As is shown in Fig. 2b, the nucleation overpotential and mass transport overpotential in the first cycle for the control sample are −170 and −76 mV, respectively, that is, the lithium deposition overpotential was calculated as −94 mV. As for the modified samples, the nucleation overpotential and mass transport overpotential are −81 and −49 mV, respectively, and the corresponding lithium deposition overpotential is thus only −32 mV, which is obviously lower than that in the control sample. The noteworthy decrease in lithium deposition overpotential demonstrates that there is no additional deposition barrier for lithium ions after the introduction of modified coating. Furthermore, originating from the good affinity between PMMA and lithium, a significant reduction in the lithium deposition overpotential was achieved.[19] In the Li–Cu half cells, the coulombic efficiency (CE) is defined as the amount of lithium stripping from the working electrodes over that depositing on it, while the Li source is excessive at the anode side. The value of CE reflects the consumption of active lithium during the actual cycling. As shown in Fig. 2c, the average coulombic efficiency of the cell with the control electrode can keep stable at 97.2% only in the first 70 cycles, and then cell failure occurs, which is mainly ascribed to the consumption accumulation of active lithium and electrolyte in the early stage during cell cycling, leading to a large interface impedance.[20,21] In the case of electrode modified by the PMMA/PVDF coating, a high and stable coulombic efficiency of 98.3% was achieved over 260 cycles. Furthermore, similar results can be observed when the testing conditions were restricted to 1 mA cm^{-2}–3 mA h cm^{-2} and 3 mA cm^{-2}–1 mA h cm^{-1}, respectively (Fig. S2b and S2c, ESI†). The bare Cu electrode presents more serious coulombic efficiency fluctuations when an increased current density is applied or lithium deposition/dissolution capacity. By contrast, cells with the modified Cu electrode still retain a stable cycling performance with average coulombic efficiencies of 97.8 and 95.6%, respectively, confirming that the flexible modified coating has a good improvement effect under the conditions of both high current density and more dramatic volume change. These remarkable improvements strongly indicate that the polymer modified coating prepared *via* electrospinning technique successfully stabilizes lithium metal anode and reduces the irreversible consumption of active lithium. To further investigate the stabilization effect of the modified electrode toward lithium deposition/stripping behavior, polarization voltage is utilized to evaluate the stability of the electrode interface in lithium metal batteries because of the accumulation of dead lithium and poor interface SEI will increase the voltage polarization.[22] Fig. 2d and Fig. S2d (ESI†) show the voltage profiles of the modified Cu/bare Cu at 1st, 10th, 50th and 150th cycles. The cell with the modified coating realizes a highly stable voltage profile with a much smaller

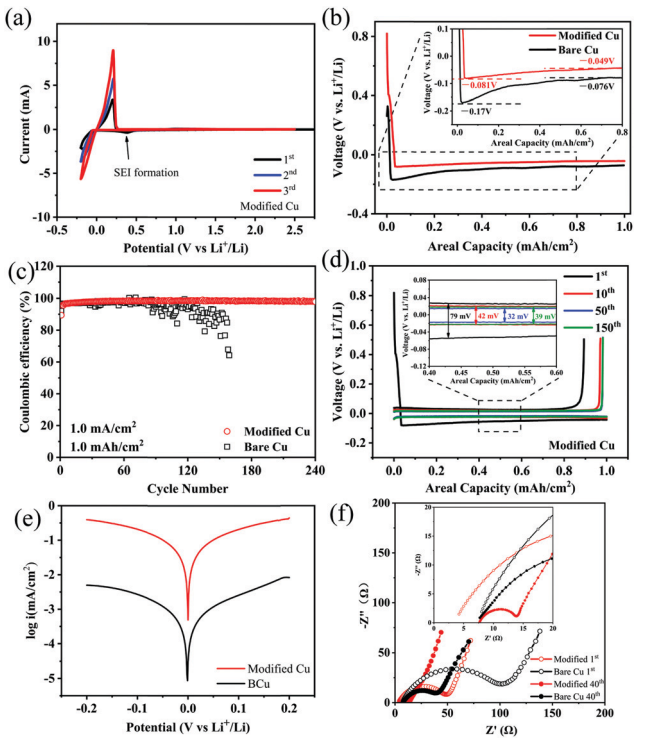

Fig. 2 Electrochemical performance comparison of Li/Cu half cells without/with a modified coating. (a) CV curve of Li/modified Cu half cell, (b) voltage–capacity curve of bare Cu/modified Cu during the first cycle discharge process, (c) the coulombic efficiency of the Li deposition/dissolution process on bare Cu/modified Cu with deposition capacity and current of 1.0 and 1.0 mA cm^{-2}, respectively, (d) voltage–capacity curve of modified Cu after different cycles. (e) Tafel plot of bare Cu/modified Cu half cells, (f) EIS curves of bare Cu and modified Cu electrode after 1st and 40th cycles.

voltage polarization compared with the control sample. After 50 cycles, the polarization voltages of the cells with bare Cu and modified Cu are 62 and 32 mV, respectively, suggesting that a PMMA/PVDF modified coating is beneficial to the formation of a stable electrode interface. By contrast, at 150 cycles, the charging voltage of the control sample exhibited obvious fluctuation, which could be ascribed to the severe interfacial fluctuation occurring on the anode induced by the poor plating/stripping behavior.[20] In addition, from the Tafel profile (Fig. 2e), a higher exchange current density of 0.112 mA cm^{-2} was obtained in the cell using modified Cu, which was significantly higher than that of the control sample (0.0017 mA cm^{-2}), confirming a better Li^+ ionic transmission in the electrode interface after being modified. Furthermore, a significantly improved electrode interface can also be confirmed by the electrochemical impedance spectra (EIS) analysis. Fig. 2d shows that no additional resistance was observed for lithium-ion migration after introducing the modified coating, which is evidently attributed to the gelatinous PMMA/PVDF modified layer with a fibrous and porous network structure reserving massive lithium migration pathways to ensure rapid Li^+ ion transmission near the electrode interface. In addition, half cells with the bare Cu electrode represent a charge transfer resistance (R_{ct}) of 94.3 Ω after the 1st cycle and 28.4 Ω at 40th cycle (Table S1, ESI†). By contrast, the charge transfer resistance of the cells using modified Cu is much smaller, which is 48.8 Ω after the first cycle and 5.98 Ω after 40 cycles, indicating a promoted SEI with much less dead lithium, which is in line with the results from the polarization voltage.[13]

Lithium deposition behavior on the bare Cu and modified Cu substrates is illustrated in Fig. 3a. Due to the unstable electrode/electrolyte interface, lithium deposition is likely to show uneven morphology on the bare Cu substrate, which will cause the growth of lithium dendrites, seriously shorten the life of lithium metal anode and reduce the coulombic efficiency. As for the polymer fiber modified Cu substrate, the abundant functional groups on the flexible polymer fibers can not only homogenize lithium ion flux by providing adhesion sites but also confine the lithium deposition behavior, thus leading to a uniform lithium deposition morphology. Fig. 3b–e are the top and cross-section SEM images of lithium deposition on bare Cu after the first cycle. After 1 mA h cm^{-2} lithium deposition at 1 mA cm^{-2}, the as-grown Li deposition presents a clear filament-like Li morphology with diameters ranging from 2 to 10 μm, known as the lithium dendrites[23] (Fig. 3b). From the cross-section view, the loose and uneven lithium deposition layer has a thickness of *ca.* 13 μm (Fig. 3c). By contrast, the deposition of lithium on the modified electrode shows a superior morphology. Firstly, it is clear that the flexible modified layer with superior mechanical robustness still retains the fibrous network structure (Fig. 3d), and less lithium is adhered, which means the diffusion of lithium ions will not be hindered and a low polarization is ensured. From the cross-section illustrated in Fig. 3e, it can be seen that lithium is deposited in a very dense form with a thickness of about 9 μm. After 40 cycles, a large amount of flocculent dead lithium can be

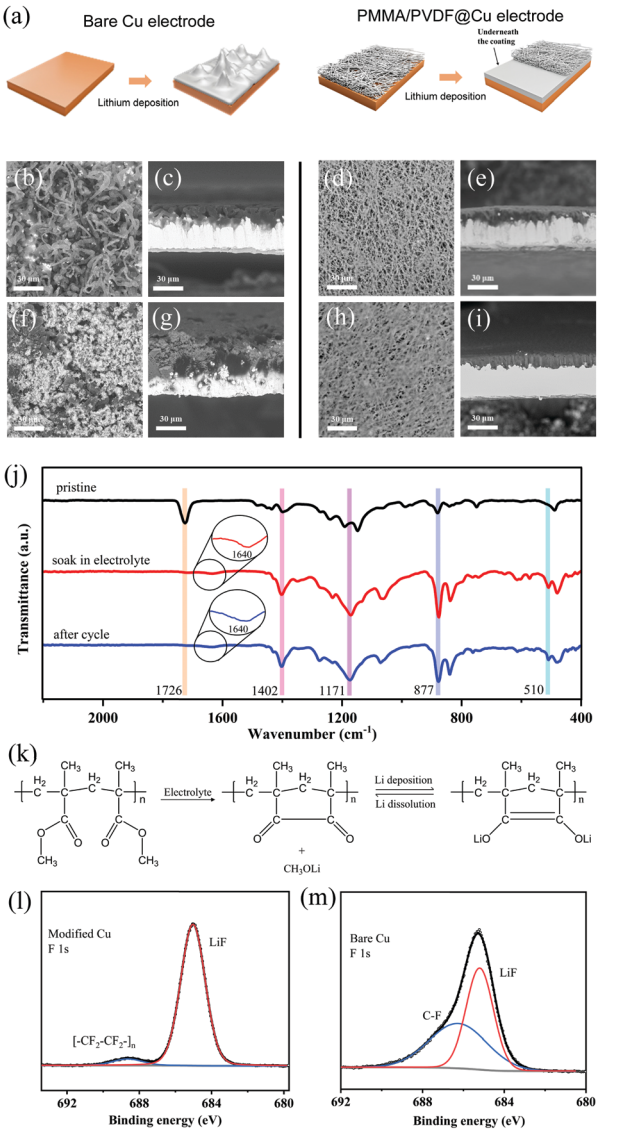

Fig. 3 Morphology and composition analysis of lithium deposition on the modified/unmodified substrates. (a) Schematic diagram of lithium deposition on electrode with/without modified coating. Top-view and cross-sectional view SEM images of lithium deposition with 1 mA h cm^{-2} capacity on (b and c) bare Cu, (d and e) modified Cu after 1 cycle, and on (f and g) bare Cu, (h and i) modified Cu after 40 cycles. (j) Comparison of the FTIR spectra of modified coating (upper) without treatment, (middle) after soaking electrolyte and (bottom) after 25 cycles. (k) Illustration of reaction process of PMMA during cycling. (l and m) The XPS high-resolution F1s spectra of modified Cu and bare Cu after cycles.

observed on the surface of the lithium deposition layer on bare Cu substrate (Fig. 3f and g), which is mainly resulting from of the massive formation of lithium dendrites in previous cycles. In the modified Cu substrate, the protective coating still maintains the fibrous network structure and the lithium deposition morphology remains flat. There are two possible reasons for this: Lithiophilic PMMA can improve the initial lithium deposition density on the substrate by chemically anchoring Li^+, so that the distribution of lithium ions will be more uniform in the subsequent process.[16] Besides, PVDF has moderate surface

energy and high dielectric constant, which are believed to promote the formation of lithium deposition with a large surface area.[15] In addition, LiF can be generated *via* the interface reaction between PVDF and lithium, which can favor a stable SEI due to its high ionic conductivity, low diffusing energy and excellent mechanical strength. As a result, the dense and uniform deposition morphology reduces the possibility for the formation of dendritic lithium, and is beneficial to enhance the cycling stability and prolong the cell lifespan.[24] As illustrated in Fig. 3j, the FTIR spectra of the modified coating at different states were investigated. Compared with the initial state discussed above, the electrospun coating after soaking in electrolyte for 12 h loses the C=O characteristic peak at 1726 cm^{-1} and forms new peaks centered at 1640 and 510 cm^{-1}, which are ascribed to the keto carbon group and the Li–O bond of the reaction product of CH_3OLi,[25] caused by the reaction between PMMA and lithium ions. The test results are consistent with the lithium anchoring process and the chemical reaction mechanism of PMMA (Fig. 3k);[26] the lithium ions trapped on the modified coating surface provide uniform nucleation sites and regulate the Li^+ ion flux during the subsequent lithium deposition process, alleviating lithium ion aggregation due to inevitable roughness of the electrode surface. Accordingly, the modified coating shows extremely low interfacial resistance and decreased lithium deposition barrier, which greatly stabilize the electrode interface and are conducive to the uniform deposition of lithium. Meanwhile, the broad split bands at 1148 and 1191 cm^{-1} also evolve to an absorption peak at around 1171 cm^{-1}, which is assigned to CF_2 stretching vibration, indicating that the compound PVDF remains stable in the modified coating and provides structural support. In the case of the PMMA/PVDF coating layer cycled in a Li/Cu half-cell for 25 cycles, no obvious change was observed in the characteristic peaks, indicating that the coating is quite stable during cycling. Fig. 3m and n present the XPS high-resolution spectra of F1s; the peaks at 685.1 and 688.6 eV for the modified Cu after cycling clearly show the existence of LiF and $[CF_2–CF_2]_n$. As for the control sample, the peaks at 685.2 and 686.3 eV can be assigned to the compound of LiF and C–F. It is obvious that an increased proportion of LiF is obtained on the modified Cu, which is essential for a uniform and stable SEI.[27,28]

The Li/Li symmetric cell tests were carried out to evaluate Li plating/stripping performance during long cycling. It is noteworthy that 4 mA h cm^{-2} Li was pre-deposited on modified Cu or bare Cu at 1.0 mA cm^{-2} (labelled as modified Cu@Li or bare Cu@Li), and the symmetric cells were assembled with two identical electrodes. As shown in Fig. 4a, on cycling at a current density of 1.0 mA cm^{-2} with a fixed capacity of 1.0 mA h cm^{-2}, the cell with the bare Cu@Li electrode presents a higher voltage overpotential due to the continuous consumption of electrolyte and the accumulation of dead lithium.[29] After 400 h, resulting from the depletion of electrolyte, the voltage hysteresis increases significantly.[30] However, the cell using the modified Cu@Li electrode exhibits stable cycling with a low overpotential (~20 mV) for over 1400 h, indicating an improved electrode interface and successful inhibition of Li dendrites.[31,32]

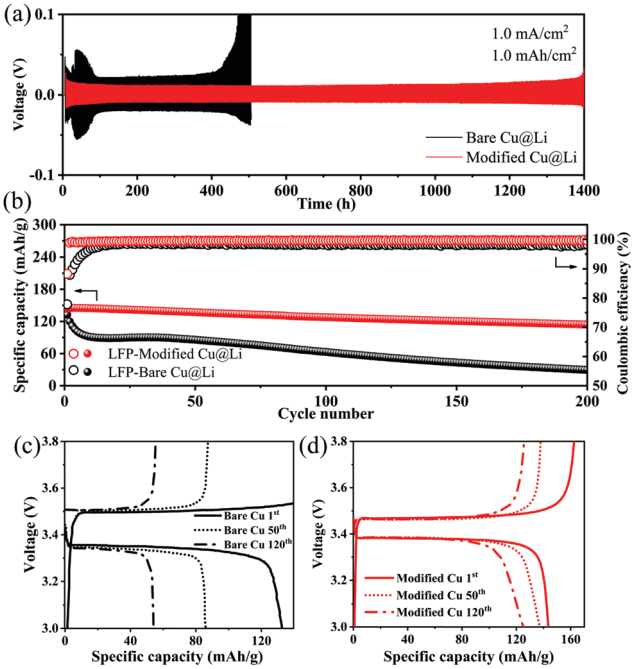

Fig. 4 Electrochemical performance of Li/Li symmetric cells and Li/$LiFePO_4$ full cells. (a) Cycle stability comparison of bare Cu@Li and modified Cu@Li at a deposition capacity and current density of 1.0 mA cm^{-2} and 1.0 mA h cm^{-2}, cycling performance (b) and voltage–capacity curves (c and d) of bare Cu@Li/LFP and modified Cu@Li/LFP.

Practical application feasibility analysis was evaluated by the galvanostatic cycling performances of full cells, which were assembled with commercial $LiFePO_4$ as the cathode, while bare/modified Cu pre-deposited with 1 mA h cm^{-2} lithium was used as the anode. In Fig. 4b, the full cells cycled at 1C were labelled as LFP-Modified Cu@Li and LFP-Bare Cu@Li, respectively. The LFP-Bare Cu@Li full cell exhibits an initial coulombic efficiency of 77.87% with a charge/discharge capacity of 170.4/132.7 mA h g^{-1}, much lower than the one using the PMMA/PVDF modified Cu@Li, whose initial coulombic efficiency is 88.31% and charge/discharge capacity is 162.5/143.5 mA h g^{-1}. In the subsequent cycling, the control sample suffered a rapid capacity degradation during the first 10 cycles, which is mainly attributed to the excessive irreversible consumption of active lithium when the lithium source is fixed. By contrast, the full cell with modified electrode retains an average coulombic efficiency of 99.5% for over 250 cycles. In addition, Fig. 4c and d show the charge–discharge profiles of two kinds of full cells at 1st, 50th, and 120th cycles. The full cell with modified Cu exhibits a much remarkedly lower voltage polarization than the control sample, confirming that the modified layer is favorable to realize stable lithium deposition/stripping behavior.[33]

3. Conclusions

In this work, a PMMA/PVDF porous coating was modified on a copper substrate directly using an electrospinning technique. It acts as an artificial coating to obtain uniform lithium deposition, protect the fragile SEI and relieve the dramatic volume

change of the anode. The affinity between the Cu substrate and the electrolyte is significantly improved due to the gel protection layer *in situ* formed on the Cu current collector, which decreases the lithium deposition barrier and the probability of dendrite growth. Moreover, the synergistic effect of lithiophilic PMMA and robust PVDF can induce a homogeneous Li^+ ion distribution and accommodate serious electrode volumetric changes during cycling, which are favorable for a stable electrode interface and uniform lithium deposition. Owing to the uniform lithium deposition and stable electrode interface achieved by the gel protection layer, superior cycling performance is achieved by the PMMA/PVDF modified electrodes in Li/Cu cells; the resulting average coulombic efficiency reaches 98.2% for over 260 cycles at 1.0 mA cm^{-2} in an ether-based electrolyte, and a stable cycling lifespan over 1400 h is achieved in a Li/Li symmetric cell at 1 mA cm^{-2} with a specific capacity of 1 mA h cm^{-2}. All in all, as an important aspect of electrode surface modification, a binary blend polymer modified coating with low interface resistance and high mechanical robustness is prepared and is proven to be effective in improving lithium metal anodes with a long cycling life.

Conflicts of interest

There are no conflicts to declare.

Acknowledgements

The authors gratefully acknowledge the financial support from the National Key R & D Program of China (2018YFB0104300), National Natural Science Foundation Committee of China (52073143, Distinguished Youth Scientists Project of 51425301, 21374021, 51573013, 51773092 and 51772147), State Key Lab Research Foundation (ZK201805, ZK201717), Jiangsu Distinguished Professorship Program (2016) and Postgraduate Research & Practice Innovation Program of Jiangsu Province (KYCX20_1072).

References

1 W. Weng, J. Lin, Y. Du, X. Ge, X. Zhou and J. Bao, *J. Mater. Chem. A*, 2018, **6**, 10168–10175.
2 Z. Zhang, Y. Du, Q.-C. Wang, J. Xu, Y.-N. Zhou, J. Bao, J. Shen and X. Zhou, *Angew. Chem., Int. Ed.*, 2020, **59**, 17504–17510.
3 X. B. Cheng, R. Zhang, C. Z. Zhao and Q. Zhang, *Chem. Rev.*, 2017, **117**, 10403–10473.
4 Z. Liu, *Acta Phys.-Chim. Sin.*, 2019, **35**, 1293–1294.
5 X. Xiong, W. Yan, C. You, Y. Zhu, Y. Chen, L. Fu, Y. Zhang, N. Yu and Y. Wu, *Front. Chem.*, 2019, **7**, 365–377.
6 M. Zhao, B.-Q. Li, H.-J. Peng, H. Yuan, J.-Y. Wei and J.-Q. Huang, *Angew. Chem., Int. Ed.*, 2020, **59**, 12636–12652.
7 X.-Q. Zhang, X. Chen, X.-B. Cheng, B.-Q. Li, X. Shen, C. Yan, J.-Q. Huang and Q. Zhang, *Angew. Chem., Int. Ed.*, 2018, **57**, 5301–5305.
8 Y. Zhong, Y. Xie, S. Hwang, Q. Wang, J. J. Cha, D. Su and H. Wang, *Angew. Chem., Int. Ed.*, 2020, **59**, 14003–14008.
9 C. Z. Zhao, P. Y. Chen, R. Zhang, X. Chen, B. Q. Li, X. Q. Zhang, X. B. Cheng and Q. Zhang, *Sci. Adv.*, 2018, **4**, eaat3446.
10 N. Li, Q. Ye, K. Zhang, H. Yan, C. Shen, B. Wei and K. Xie, *Angew. Chem., Int. Ed.*, 2019, **58**, 18246–18251.
11 X. Ke, Y. Cheng, J. Liu, L. Liu, N. Wang, J. Liu, C. Zhi, Z. Shi and Z. Guo, *ACS Appl. Mater. Interfaces*, 2018, **10**, 13552–13561.
12 A. A. Assegie, J. H. Cheng, L. M. Kuo, W. N. Su and B. J. Hwang, *Nanoscale*, 2018, **10**, 6125–6138.
13 A. A. Assegie, C. C. Chung, M. C. Tsai, W. N. Su, C. W. Chen and B. J. Hwang, *Nanoscale*, 2019, **11**, 2710–2720.
14 B. Liang, S. Q. Tang, Q. B. Jiang, C. S. Chen, X. Chen, S. L. Li and X. H. Yan, *Electrochim. Acta*, 2015, **169**, 334–341.
15 J. Lopez, A. Pei, J. Y. Oh, G. N. Wang, Y. Cui and Z. Bao, *J. Am. Chem. Soc.*, 2018, **140**, 11735–11744.
16 Z. Liang, G. Zheng, C. Liu, N. Liu, W. Li, K. Yan, H. Yao, P. C. Hsu, S. Chu and Y. Cui, *Nano Lett.*, 2015, **15**, 2910–2916.
17 S. Liang, W. Yan, X. Wu, Y. Zhang, Y. Zhu, H. Wang and Y. Wu, *Solid State Ionics*, 2018, **318**, 2–18.
18 T. T. Beyene, B. A. Jote, Z. T. Wondimkun, B. W. Olbassa, C. J. Huang, B. Thirumalraj, C. H. Wang, W. N. Su, H. Dai and B. J. Hwang, *ACS Appl. Mater. Interfaces*, 2019, **11**, 31962–31971.
19 X. Hu, P. Xu, S. Deng, J. Lei, X. Lin, Q. Wu, M.-S. Zheng and Q.-F. Dong, *J. Mater. Chem. A*, 2020, **8**, 17056–17064.
20 Y. M. Liu, X. Y. Qin, S. Q. Zhang, L. H. Zhang, F. Y. Kang, G. H. Chen, X. F. Duan and B. H. Li, *J. Mater. Chem. A*, 2019, **7**, 13225–13233.
21 K. Yan, B. Sun, P. Munroe and G. Wang, *Energy Storage Mater.*, 2018, **11**, 127–133.
22 G. Zheng, S. W. Lee, Z. Liang, H. W. Lee, K. Yan, H. Yao, H. Wang, W. Li, S. Chu and Y. Cui, *Nat. Nanotechnol.*, 2014, **9**, 618–623.
23 J. Steiger, G. Richter, M. Wenk, D. Kramer and R. Mönig, *Electrochem. Commun.*, 2015, **50**, 11–14.
24 Y. Zhao, D. Wang, Y. Gao, T. Chen, Q. Huang and D. Wang, *Nano Energy*, 2019, **64**, 103893.
25 Y. Guo, Y. Ouyang, D. Li, Y. Wei, T. Zhai and H. Li, *Energy Storage Mater.*, 2019, **16**, 203–211.
26 Y. Wang, L. Zhang, L. Zhang, F. Zhang, P. He, H. Zheng and H. Zhou, Advanced Energy, *Materials*, 2016, **6**, 1601375.
27 T. T. Hagos, B. Thirumalraj, C. J. Huang, L. H. Abrha, T. M. Hagos, G. B. Berhe, H. K. Bezabh, J. Cherng, S. F. Chiu, W. N. Su and B. J. Hwang, *ACS Appl. Mater. Interfaces*, 2019, **11**, 9955–9963.
28 S. Sun, S. Myung, G. Kim, D. Lee, H. Son, M. Jang, E. Park, B. Son, Y.-G. Jung, U. Paik and T. Song, *J. Mater. Chem. A*, 2020, **8**, 17229–17237.
29 Y. He, H. Xu, J. Shi, P. Liu, Z. Tian, N. Dong, K. Luo, X. Zhou and Z. Liu, *Energy Storage Mater.*, 2019, **23**, 418–426.
30 J. Xiao, P. Zhai, Y. Wei, X. Zhang, W. Yang, S. Cui, C. Jin, W. Liu, X. Wang, H. Jiang, Z. Luo, X. Zhang and Y. Gong, *Nano Lett.*, 2020, **20**, 3911–3917.
31 S. Liu, L. Deng, W. Guo, C. Zhang, X. Liu and J. Luo, *Adv. Mater.*, 2019, **31**, e1807585.
32 S. Liu, X. Xia, Y. Zhong, S. Deng, Z. Yao, L. Zhang, X.-B. Cheng, X. Wang, Q. Zhang and J. Tu, *Adv. Energy Mater.*, 2018, **8**, 1702322.
33 W. Zhang, Q. Yi, S. Li and C. Sun, *J. Power Sources*, 2020, **450**, 227710.